Phase (Liquid/Solid) Dependence of the Normal Spectral Emissivity for Iron, Cobalt, and Nickel at Melting Points

Hiromichi Watanabe,[1–3] Masahiro Susa,[1] Hiroyuki Fukuyama,[4] and Kazuhiro Nagata[4]

Normal spectral emissivities of liquid and solid Fe, Co, and Ni have been determined at their melting points at wavelengths from 650 to 800 nm and from 1000 to 1900 nm using an apparatus that consists of a cold crucible and diffraction grating spectroscopes. For all three metals, the emissivities of the liquid phases are slightly larger than those of the solid phases both in the visible and near-infrared regions. For iron, the near-infrared emissivities decreased progressively with each additional measurement series and settled down after three series. A possible explanation to this behavior is offered. The present results for iron were assessed by comparisons with previously reported results and with predictions based upon the Hagen–Rubens relation for the ratio of the emissivity of the liquid to that of the solid ($\varepsilon_{\text{Liquid}}/\varepsilon_{\text{Solid}}$). The measured emissivities for all three metals are in good agreement with previous results at and near the melting point. The results for $\varepsilon_{\text{Liquid}}/\varepsilon_{\text{Solid}}$ in the near-infrared region demonstrate that the phase (liquid/solid) dependence of the infrared emissivity is consistent with that of the dc resistivity for all the metals at their melting points.

---

[1] Department of Metallurgy and Ceramics Science, Tokyo Institute of Technology, 2-12-1 Ookayama, Meguro-ku, Tokyo 152-8552, Japan.

[2] Present address: Thermophysical Properties Section, National Metrology Institute of Japan, AIST, 1-1-1 Umezono, Tsukuba, Ibaraki 305-8563, Japan.

[3] To whom correspondence should be addressed. E-mail: hiromichi-watanabe@aist.go.jp

[4] Department of Chemistry and Materials Science, Tokyo Institute of Technology, 2-12-1 Ookayama, Meguro-ku, Tokyo 152-8552, Japan.

1. INTRODUCTION

The recent development of containerless processes requires emissivity data for molten metals, since they are essential for temperature measurements using radiation thermometers and computer simulations for heat transfer in high-temperature material processes. It is well known that the spectral emissivities of molten metals show moderate temperature dependence. Because of this, emissivity data for materials at their melting points have been used as standard values for the liquids. Therefore, it is important to have accurate values of spectral emissivity for metals at their melting points. In addition, at the melting point, solid and liquid phases coexist, and, thus, the emissivities of the liquid phase should be distinguished from those of the solid phase. The phase (liquid/solid) dependence of the emissivity for metals at their melting points is very interesting from a scientific point of view, since the possible difference between the emissivities of liquid and solid phases is related to that between the electronic structures of the liquid and solid.

There have been many literature data of spectral emissivities and optical constants for iron [1–12], cobalt [2, 5, 7, 10, 13], and nickel [1, 2, 5, 7, 9, 11, 14, 15] at and near their melting points. However, significant discrepancies exist among the previous results on the phase dependence of the emissivity of the metals at their melting points. In 1914 Bidwell [1] measured spectral emissivities of liquid and solid iron and nickel at their melting points at 660 nm. He found that there are no differences between the emissivities of liquid and solid phases at the melting point for both iron and nickel. In 1915 Burgess and Waltenberg [2] reported that the emissivities of cobalt and nickel slightly increase on melting (from 0.36 to 0.37 for Co and Ni at 650 nm and from 0.44 to 0.46 for Ni at 550 nm), but that of iron (0.37 at 650 nm) is constant with the melting transition. Miller [5] reported that there are small differences between the emissivities deduced from the optical constants of liquid and solid cobalt at the melting point. Shvarev et al. [8] measured the optical constants of iron at temperatures of 293, 1673, and 1873 K over a wavelength range from 600 to 3390 nm, and observed slight changes in the optical constants during melting of iron. However, emissivity measurements of the three transition metals at their melting points using electromagnetic levitation-heating [7] and rapid resistive self-heating [10, 14, 15] have indicated that there are no sudden changes in spectral emissivity of any of the three metals at the solid-to-liquid transition. Dubrovinsky and Saxena [12] have recently measured normal spectral emissivities of solid iron at the melting point in the visible and infrared regions using a heating-wire technique and multiwavelength spectral radiometry. Their data are much smaller than other previously

reported data that have been considered to correspond to the emissivities for the liquid or the mixture of the liquid and solid at the melting point. Therefore, it has not yet been made clear whether spectral emissivities of the three transition metals change at the solid-to-liquid transition.

The purposes of this work are (1) to present reliable data of normal spectral emissivities for iron, cobalt, and nickel in liquid and solid states at their melting points in the visible and near-infrared regions, and (2) to investigate the phase (liquid/solid) dependence of the spectral emissivity for the transition metals at their melting points. To measure the emissivities of liquid and solid phases separately, a cold crucible was utilized for heating the sample. The cold crucible can melt metals inductively and hold the molten metals by electromagnetic force. The containerless process in the cold crucible has provided two advantages for the measurements of the emissivities of metallic materials during the liquid-to-solid transition, as follows: (1) the solidification front moves on the sample surface slowly enough to allow measurements of the emissivities of liquid and solid phases separately and (2) a very clean, smooth surface of the solid sample is realized by virtue of the resolidification process. Using the cold crucible, we have measured normal spectral emissivities of Cu [16–18], Ag [17, 18], Au [17, 18], and Si [19] in liquid and solid states at their melting points. These previous studies have demonstrated sufficient performance of the apparatus for accurate determinations of both emissivities at the melting point.

2. EXPERIMENTAL

The experimental methods used in the present study were essentially the same as those used in our previous studies [16–19]. Figure 1 shows the experimental setup for recording the normal spectral radiance emitted from the sample. The purity of the sample used in this study was 99.99 mass% for Fe and Ni and 99.98 mass% for Co. Each sample was machined into a cylinder (10 to 20 mm in diameter and 5 to 20 mm in length). The cylindrical samples were cleaned in alcohol and acetone prior to the experiments. The sample was placed on a sintered plate made of magnesia powder with a purity of 99.9 mass% and heated using the cold crucible. To avoid surface oxidation of the sample, the experiments were conducted in a flow of argon gas containing 10 pct hydrogen for Fe and in a flow of pure argon gas deoxidized with Mg ribbons at about 750 K for Co and Ni, and the total pressure was kept at atmospheric pressure. For the experiments on Co and Ni, sponge zirconium was also used as an oxygen getter, which was contained in an alumina crucible and placed under the magnesia plate. The alumina crucible was inserted in a graphite crucible that served as a susceptor to heat the zirconium.
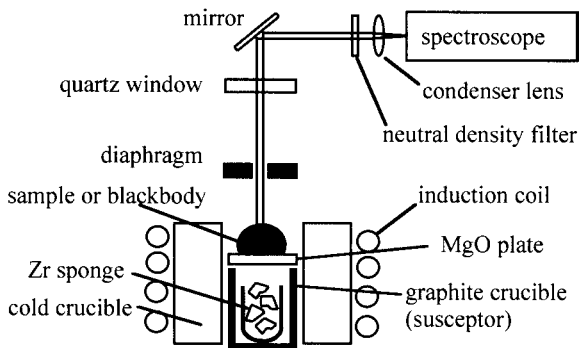
Fig. 1. Schematic diagram of experimental setup.

The normal spectral radiance of the sample was measured with two types of spectroscopes with grating monochromators covering the ranges from 650 to 800 nm and from 1000 to 1900 nm, the detectors of which were a photomultiplier tube and a PbS photoconductive cell, respectively. When the sample was melted, the diameter of the melt surface was approximately 20 mm. To obtain only the normal radiation from the heated sample, a diaphragm (5 mm in diameter and 20 mm in length) was placed at a distance of approximately 50 mm vertically above the melt surface. After passing the diaphragm, the normal radiation emitted from a circular region of approximately 5 mm in diameter in the center of the sample surface was transmitted to the spectroscope by a combination of a mirror and a condenser lens. The length of the optical path between the sample surface and the entrance slit of the monochromator was approximately 500 mm. The spectroscope was calibrated to convert the output voltage from the detector into the spectral radiance with a fixed-point blackbody of copper. The calibration procedures are also described in our previous papers [16, 19]. The spectral radiance from the samples at their melting points is much greater than that from the blackbody cavity at the melting point of copper. Therefore, neutral density filters, which reduce the intensity of the light introduced into the detectors, were placed in front of the spectroscope to make the light intensity measurable. Prior to the emissivity measurements, spectral transmittances of the filters were measured using the spectroscopes calibrated with the fixed-point blackbody of copper.

A pair of spectral emissivities of the liquid and solid at the melting point at a single wavelength was obtained during one freezing transition of the sample. The emissivity measurement on freezing was carried out from 650 to 800 nm at intervals of 50 nm and from 1000 to 1900 nm at intervals of 100 nm with the spectroscopes. After the measurements, the root-mean-

square roughness of the resolidified sample surface was measured to be negligibly small (less than 15 nm) using a profile measurement microscope.

3. RESULTS

3.1. Normal Spectral Emissivity of Iron at Melting Point

Normal spectral emissivities of liquid and solid iron at the melting point (1808 K) are plotted as a function of wavelength in Fig. 2. Unfilled circles and triangles represent the averages of five measured values for the emissivities of the liquid and solid, respectively. The error bars of the symbols in the visible region denote the standard deviation of the five measured values from the average. No systematic deviation was observed among the data obtained in the five measurement runs for the visible region. In the wavelength range from 1000 to 1900 nm, four measurement runs were carried out for one sample. In contrast to the visible emissivities measured, the infrared emissivities exhibited significant deviations between the data obtained in the first two runs and in the last two runs. Filled
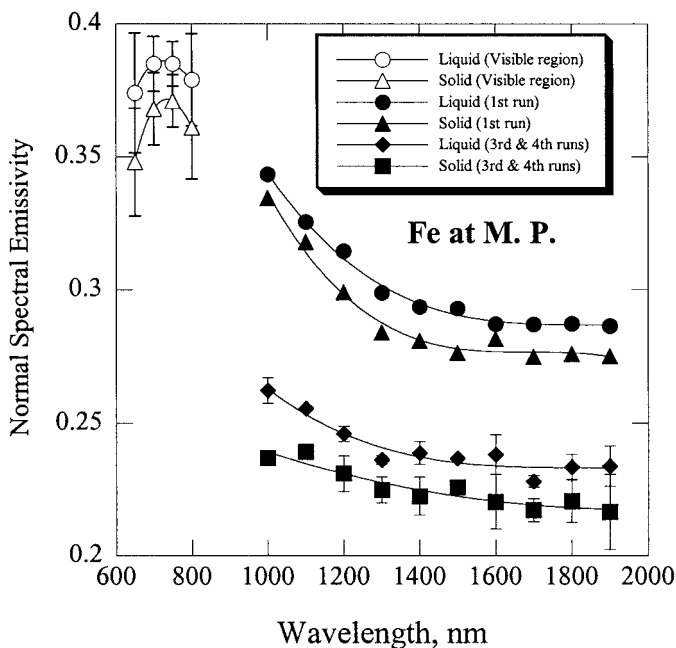

Fig. 2. Experimental results of normal spectral emissivities for liquid and solid iron at melting point.

circles and triangles in Fig. 2 represent the infrared emissivities obtained in the first run for the liquid and solid, respectively. Diamonds and squares represent the averages of the infrared emissivities obtained in the third and fourth runs for the liquid and solid, respectively. The error bars of the diamonds and squares denote the difference between the two emissivity values obtained in the third and fourth runs. All the infrared emissivities obtained in the four runs are illustrated for the liquid and solid in Figs. 3 and 4, respectively. These figures illustrate that both the emissivities of the liquid and solid decreased with each additional measurement run and settled down after three runs. We consider that the emissivities obtained during the first run correspond to intrinsic emissivity values for iron at the melting point, based upon comparisons with the previously reported results and with the prediction based upon the Hagen–Rubens relation for the ratio of the emissivity of the liquid to that of the solid ($\varepsilon_{\text{Liquid}}/\varepsilon_{\text{Solid}}$). The two reasons for selecting the first run and a possible explanation for the decrease in the emissivity will be described in Section 4. The solid curves on Fig. 2 are drawn according to fitting polynomial functions for the emissivities, for which the functions have been obtained by regression of the
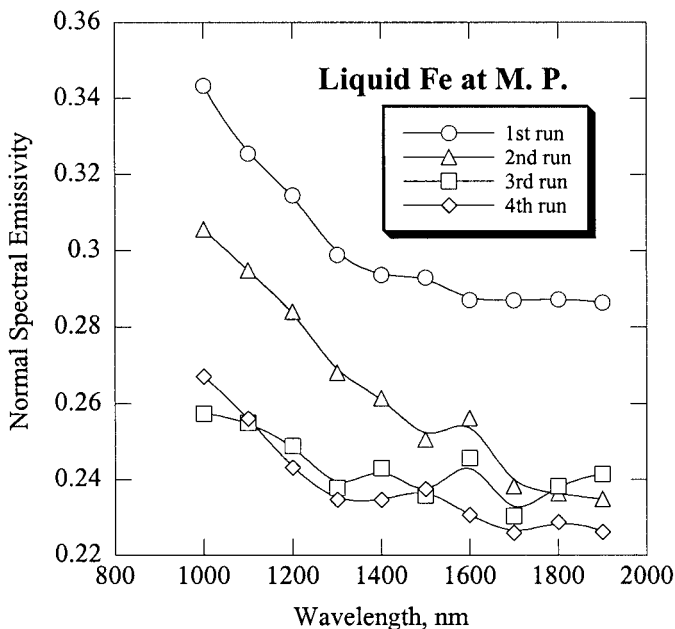

Fig. 3. Change in emissivity with number of measurement run for liquid iron heated in a flow of hydrogen.
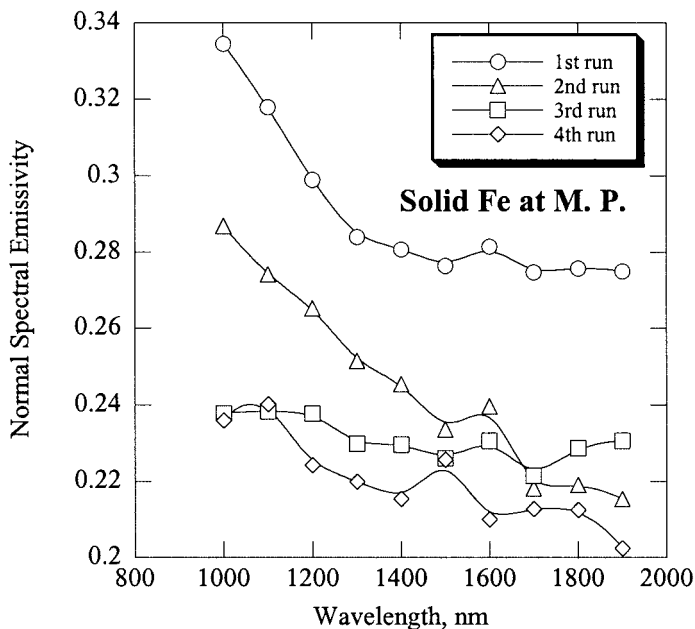
Fig. 4. Change in emissivity with number of measurement run for solid iron heated in a flow of hydrogen.

Table I. Coefficients of M_i in Eq. (1) obtained by Regression of Measured Emissivity with Polynomial Function

M_i	Fe		Co		Ni	
	liquid	solid	liquid	solid	liquid	solid
			Visible region			
M_0	-3.045	-3.279	5.9419×10^{-2}	0.59589	-0.11645	0.23112
M_1	1.2973×10^{-2}	1.2817×10^{-2}	8.7331×10^{-4}	-6.7977×10^{-4}	1.4154×10^{-3}	3.9048×10^{-4}
M_2	-1.62×10^{-5}	-1.46×10^{-5}	-7.0446×10^{-7}	3.6485×10^{-7}	-1.0496×10^{-6}	-3.4115×10^{-7}
M_3	6.6667×10^{-9}	5.3334×10^{-9}				
			Infrared region			
M_0	0.90125	1.1506	0.48825	0.42085	0.50651	0.49034
M_1	-1.0098×10^{-3}	-1.5491×10^{-3}	-2.7572×10^{-4}	-1.9746×10^{-4}	-2.8023×10^{-4}	-2.9084×10^{-4}
M_2	5.5366×10^{-7}	9.1535×10^{-7}	7.7607×10^{-8}	4.9059×10^{-8}	6.7896×10^{-8}	7.0119×10^{-8}
M_3	-1.0128×10^{-10}	-1.8033×10^{-10}				

average emissivities or the emissivity obtained in the first run to the following expression:

$$\varepsilon(\lambda) = \sum_{i=0}^{3} M_i \lambda^i \tag{1}$$

where λ is the wavelength in nm and M_i's are the coefficients given in Table I.

3.2. Normal Spectral Emissivities of Cobalt and Nickel at Melting Points

Figures 5 and 6 show the present results of normal spectral emissivities of liquid and solid cobalt and nickel at their melting points (Co; 1768 K and Ni; 1729 K), respectively. The measurements for the emissivities from 650 to 800 nm and from 1000 to 1900 nm were both repeated twice. Circles and triangles on the figures represent the averages of the emissivities measured in the two runs for the liquid and solid, respectively. The unfilled
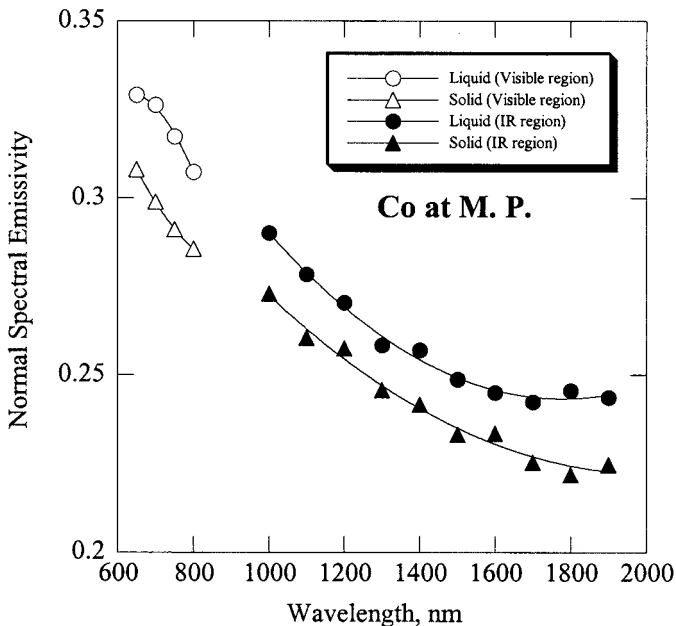

Fig. 5. Experimental results of normal spectral emissivities for liquid and solid cobalt at melting point.
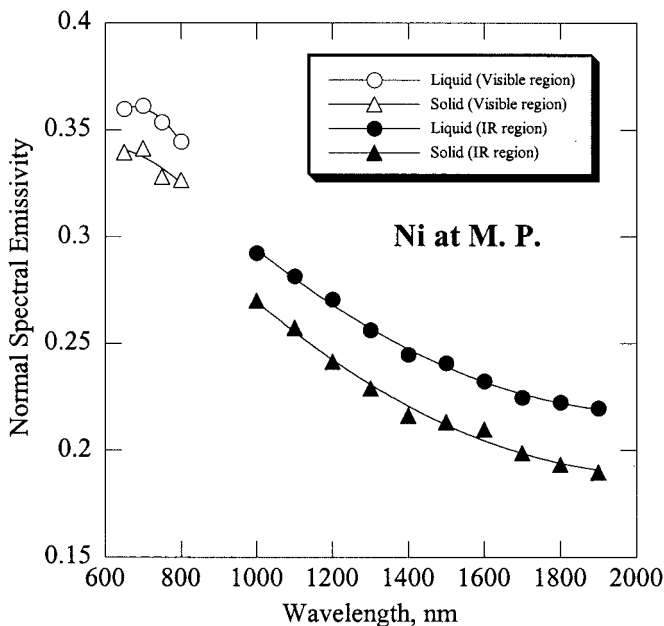
Fig. 6. Experimental results of normal spectral emissivities for liquid and solid nickel at melting point.

and filled symbols correspond to the results obtained using the spectroscopes for the visible and infrared regions, respectively. In the cases of cobalt and nickel, no systematic deviations were observed between the results obtained in the two runs, and differences between the two measured values at the wavelengths investigated were as small as the magnitude of the symbols. The solid curves on the figures represent fitting polynomial functions for the average emissivities, whose coefficients are given in Table I together with those for iron.

4. DISCUSSION

4.1. Uncertainty of Emissivity

The major sources of the uncertainty of the measured emissivity are as follows: (1) the calibration of spectroscopes, (2) the calibration of neutral density filters, and (3) changes in the geometry of the sample surface caused by the oscillation of the molten sample and the phase transition. Relative values of the individual uncertainties and the combined standard

Table II.   Relative Values of Individual Uncertainties and Combined Standard Uncertainties of Emissivity

| Uncertainty sources | Region | Relative uncertainties (%) | | | | | |
		Liquid Fe	Solid Fe	Liquid Co	Solid Co	Liquid Ni	Solid Ni
Calibration of	Visible	2.87	2.87	2.87	2.87	2.87	2.87
spectroscopes	Infrared	2.31	2.31	2.31	2.31	2.31	2.31
Calibration of							
neutral density filters		4	4	4	4	4	4
Change in geometry	Visible	3.86	4.39	0.215	0.254	0.316	0.282
of sample surface	Infrared	1.54	2.61	0.238	0.403	0.748	1.13
Relative combined	Visible	6.26	6.60	4.93	4.93	4.93	4.93
standard uncertainty (%)	Infrared	4.87	5.31	4.63	4.64	4.68	4.76

uncertainties of the emissivity are listed in Table II. The standard uncertainties associated with the first factor for the visible and infrared regions were estimated to be 2.87 and 2.31%, respectively, which correspond to the standard deviations of calibration results with the fixed point of copper. The standard uncertainty associated with the second factor was estimated to be 4%, which corresponds to the standard deviation of the results for the measurements of the spectral transmittance of the filters. The standard uncertainties due to the third factor were roughly estimated as the standard deviations of the two or five values obtained during different runs from the average. For the infrared emissivity of iron, the standard deviation of the two values obtained during the third and fourth runs from the average was considered to be the third uncertainty. The combined standard uncertainties were estimated from the square root of the sum of the squares of the individual uncertainties.

4.2. Comparison with Previously Reported Data for Iron

Figure 7 shows a comparison of the present and previous data [1–12] of the emissivity for liquid and solid iron at and near the melting point. The dotted lines indicate the fitting curves calculated from Eq. (1). The error bars correspond to the combined standard uncertainty of the present data. Inspection of the figure shows that the present results are in good agreement with the previously reported data, except for two previous results [3, 12]. The relatively large emissivity value [3] at 650 nm was obtained using a classical method; the sample was contained in a refractory
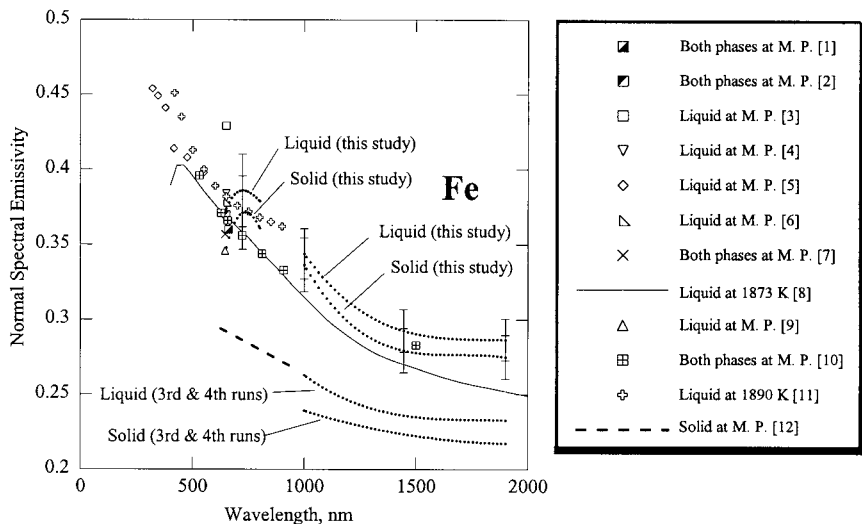
Fig. 7. Comparison of present and previous experimental data for iron at and near melting point.

crucible, and the radiance and true temperatures of the sample were measured using a single-wavelength pyrometer and a thermocouple or a blackbody cavity located near the sample, respectively. In their experiment, a silica tube was located above the sample surface to collect the normal radiation emitted from the surface. This kind of optical geometry would lead to stray radiation being emitted from the crucible and tube and then causing large systematic errors, as pointed out by d'Entremont [4]. On the other hand, the relatively small emissivity data at wavelengths from 630 to 900 nm were measured by Dubrovinsky and Saxena [12] using a novel method; the sample was heated using a metal wire (0.35 mm in diameter) with a hole (0.025 mm in diameter) in which the sample was placed, and the emissivity and temperature of the sample were measured by comparison with the intensity of thermal radiation from the reference material (rhenium) and by *in situ* x-ray observation of thermal expansion for the wire or visual observations of melting transitions for some materials, respectively. No adequate explanation for the relatively low values can be offered from the available information of the novel method. It is only suggested that the surfaces of their samples were completely or partly covered with some oxides having relatively small emissivity values. In their experiment, iron samples, which contained minute amounts of impurities, were heated in a flow of argon gas containing no deoxidizer such as hydrogen. The Ellingham diagram [20] shows that many elements are

easily oxidized at high temperatures such as the melting point of iron if there is no deoxidizer in the atmosphere.

4.3. Decrease of Emissivity for Iron with Successive Measurement Runs

The infrared emissivities observed in the present study decreased with each additional measurement run and then settled down after three runs. It is interesting to note that the average emissivities for the third and fourth runs are in fairly good agreement with the extrapolated values of the previous data of Dubrovinsky and Saxena [12] to the infrared region, as shown in Fig. 7. This suggests that the surface condition of the sample during the third and fourth runs was similar to that of the sample used by Dubrovinsky and Saxena, i.e., some oxide film with a low emissivity was present on the sample surface. In the present study, a sintered magnesia plate was used as the contact material. Normal spectral emissivities of polycrystalline magnesia at 1600 K have been reported to be 0.227, 0.196,
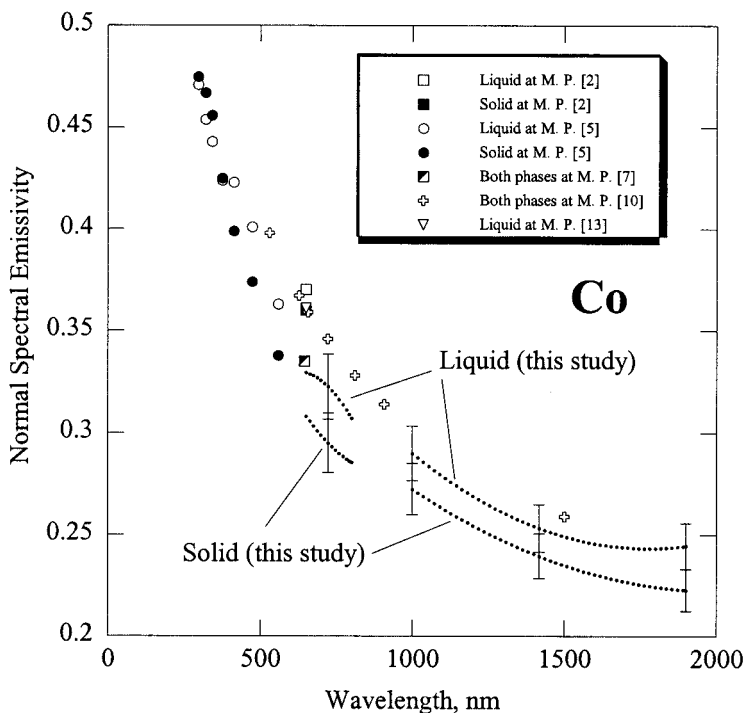

Fig. 8. Comparison of present and previous experimental data for cobalt at and near melting point.

and 0.151 for wavelengths of 1000, 1500, and 2000 nm, respectively [21]. These values being smaller than the iron emissivities indicate that the presence of magnesia on the iron sample decreases the apparent emissivity. Accordingly, the decrease in the infrared emissivity is because a thin magnesia film gradually covered the measured area of the sample. On the other hand, the visible emissivities obtained during five measurement runs did not exhibit such a behavior. This implies that the possible thin magnesia layer can transmit the visible light emitted from the iron sample but not the infrared light.

4.4. Comparison with Previously Reported Data for Cobalt and Nickel

The present and previous data for the emissivity of cobalt and nickel are illustrated in Figs. 8 and 9, respectively. The dotted lines on the figures indicate the fitting curves calculated from Eq. (1). The error bars correspond to the combined standard uncertainty of the present data. The previous results for cobalt [2, 5, 7, 10, 13] and nickel [1, 2, 5, 7, 9, 11, 14, 15]
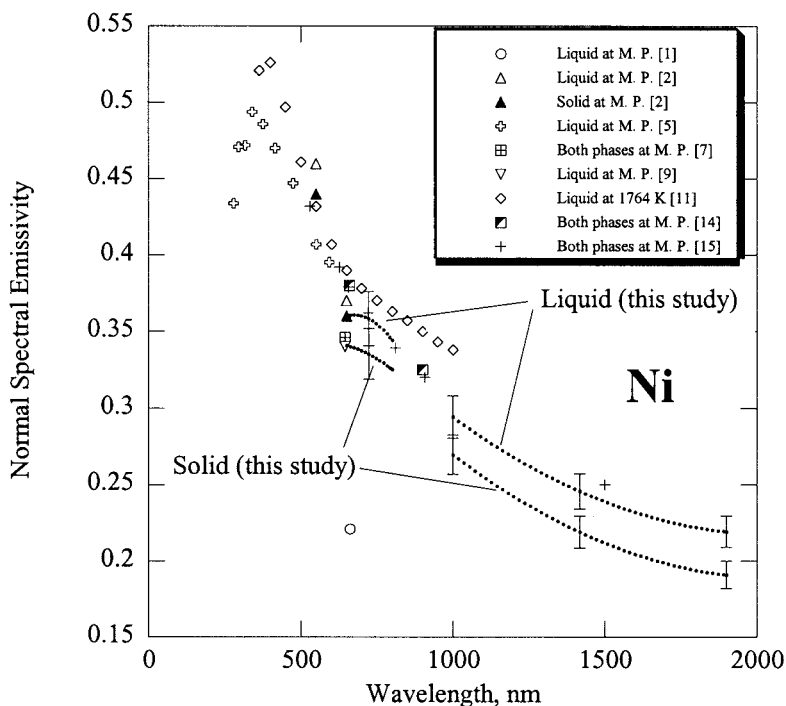

Fig. 9. Comparison of present and previous experimental data for nickel at and near melting point.

are in fairly good agreement with the present data for the liquid phases, except for one classical experimental datum [1] for liquid nickel. This implies that sample surfaces investigated in the previous studies were completely or mostly covered with the liquid phases during the measurements. The differences between the emissivities obtained by Miller [5] for liquid and solid cobalt in the visible region are as large as those observed in the present study, which confirms the existence of the difference in the emissivity between the liquid and solid phases at the melting point.

4.5. Phase (Liquid/Solid) Dependence of Emissivity

The present results demonstrate that the normal spectral emissivities of iron, cobalt, and nickel slightly increase on the solid-to-liquid transition at all the wavelengths investigated. For the visible region, some researchers have reported that there are slight differences in emissivity between liquid and solid for iron [8], cobalt [2, 5], and nickel [2]. However, there have been no experimental studies on the phase (liquid/solid) dependence of the emissivity in the infrared region for the three transition metals. In this section, the observed differences in the infrared emissivity between the liquid and solid are assessed by comparing with the differences in the dc resistivity between the liquid and solid. In the far infrared region, the spectral emissivity (ε_λ) of metals at a wavelength (λ) is related to the dc resistivity (ρ) by the Hagen–Rubens relation:

$$\varepsilon_\lambda = 0.365 \sqrt{\rho/\lambda}. \tag{2}$$

Accordingly, the ratio of $\varepsilon_{\text{Liquid}}/\varepsilon_{\text{Solid}}$ in the far infrared region can be estimated using the following relation:

$$\varepsilon_{\text{Liquid}}/\varepsilon_{\text{Solid}} = \sqrt{\rho_{\text{Liquid}}/\rho_{\text{Solid}}} \tag{3}$$

where ρ_{Liquid} and ρ_{Solid} are the dc resistivities of the liquid and solid phases at the melting point, respectively. Figure 10 shows comparisons between the measured ratios of $\varepsilon_{\text{Liquid}}/\varepsilon_{\text{Solid}}$ in the near infrared region and those estimated from the experimental data [22] of ρ_{Liquid} and ρ_{Solid} for iron, cobalt, and nickel at their melting points. Solid lines on the figure are obtained using the emissivities calculated from Eq. (1) for the liquid and solid. The long-dashed line represents the ratio of $\varepsilon_{\text{Liquid}}/\varepsilon_{\text{Solid}}$ obtained in the third and fourth runs for iron. Diamonds located at 2000 nm represent the ratios of $\varepsilon_{\text{Liquid}}/\varepsilon_{\text{Solid}}$ calculated from Eq. (3). Inspection of this figure shows that for all three metals the extrapolated values of the measured $\varepsilon_{\text{Liquid}}/\varepsilon_{\text{Solid}}$ to the far infrared region are in fairly good agreement with the
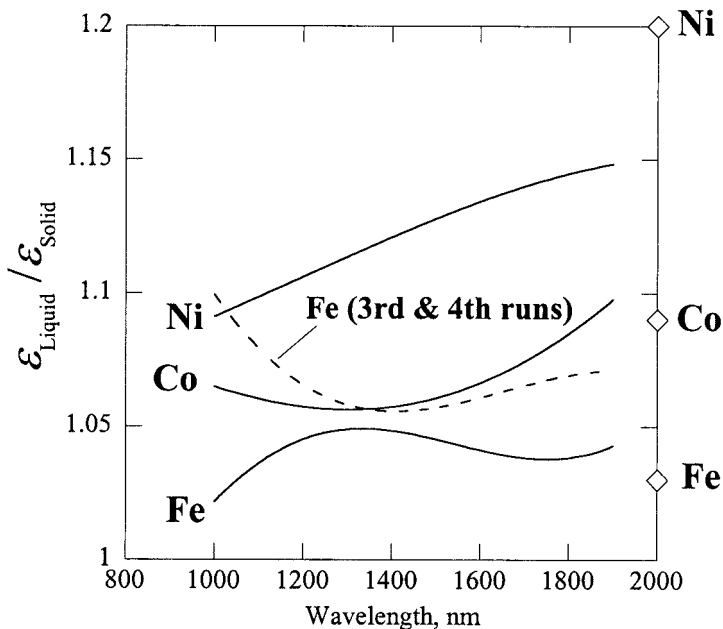
Fig. 10.   Ratios of infrared emissivity of liquid to that of solid ($\varepsilon_{\text{Liquid}}/\varepsilon_{\text{Solid}}$) for Fe, Co, and Ni at their melting points.

ratios predicted based upon the Hagen–Rubens relation. These agreements support the existence of a difference in infrared emissivity between the liquid and solid at the melting point for the three metals. Compared with the ratios of $\varepsilon_{\text{Liquid}}/\varepsilon_{\text{Solid}}$ obtained in the first run for iron, the ratios obtained in the third and fourth runs are in poor agreement with those based upon the Hagen–Rubens relation. This confirms that the emissivity data obtained for iron in the first run are more reliable than those obtained in the third and fourth runs.

5. CONCLUSIONS

Normal spectral emissivities have been determined for liquid and solid iron, cobalt, and nickel at their melting points at wavelengths from 650 to 800 nm and from 1000 to 1900 nm. The main results are given below.

- For all three metals, the emissivities of the liquid are slightly larger than those of the solid in the visible and near-infrared regions.
- The emissivities measured for all the three metals are in good agreement with most previously reported data at and near the melting point.

- The infrared emissivities of iron at the melting point could be easily affected by minute impurities on the sample surface.
- The ratios of $\varepsilon_{\text{Liquid}}/\varepsilon_{\text{Solid}}$ measured for all the metals in the near-infrared region are in good agreement with those predicted from the differences in dc resistivity between the liquids and solids at their melting points.

ACKNOWLEDGMENTS

REFERENCES

1. C. C. Bidwell, *Phys. Rev.* **3**:439 (1914).
2. G. K. Burgess and R. G. Waltenberg, *Bull. Bur. Stand.* **11**:591 (1915).
3. M. N. Dastur and N. A. Gokcen, *AIME Trans.* **185**:665 (1949).
4. J. C. d'Entremont, *Trans. AIME* **227**:482 (1963).
5. J. C. Miller, *Phil. Mag.* **20**:1115 (1969).
6. J. A. Treverton and J. L. Margrave, *J. Chem. Thermodyn.* **3**:473 (1971).
7. D. W. Bonnell, J. A. Treverton, A. J. Valerga, and J. L. Margrave, in *Temperature, Its Measurement and Control in Science and Industry*, Vol. 4, Part 1, H. H. Plumb, ed. (Instrument Society of America, Pittsburg, Pennsylvania, 1972), pp. 483–487.
8. K. M. Shvarev, V. S. Gushchin, and B. A. Baum, *Teplofiz. Vys. Temp.* **16**:520 (1977).
9. P. Ratanapupech and R. G. Bautista, *High Temp. Sci.* **14**:269 (1981).
10. E. Kaschnitz, J. L. McClure, and A. Cezairliyan, *High Temp., High Press.* **29**:103 (1997).
11. S. Krishnan, K. J. Yugawa, and P. C. Nordine, *Phys. Rev. B* **55**:8201 (1997).
12. L. S. Dubrovinsky and S. K. Saxena, *High Temp., High Press.* **31**:393 (1999).
13. J. A. Treverton and J. L. Margrave, *J. Phys. Chem.* **75**:3737 (1971).
14. A. Cezairliyan, A. P. Miiller, F. Righini, and A. Rosso, *High Temp., High Press.* **23**:325 (1991).
15. A. Cezairliyan and J. L. McClure (unpublished data, which are referenced in Ref. 11).
16. H. Watanabe, M. Susa, and K. Nagata, *Metall. Mater. Trans. A.* **28**:2507 (1997).
17. H. Watanabe, M. Susa, H. Fukuyama, and K. Nagata, *Int. J. Thermophys.* **24**:223 (2003).
18. H. Watanabe, M. Susa, H. Fukuyama, and K. Nagata, submitted to *Int. J. Thermophys.*
19. H. Watanabe, M. Susa, H. Fukuyama, and K. Nagata, *High Temp., High Press.* **31**:587 (1999).
20. F. D. Richardson and J. H. E. Jeffes, *J. Iron Steel Inst.* **160**:261 (1948).
21. Y. S. Touloukian and D. P. DeWitt, eds., *Thermophysical Properties of Matter*, Vol. 8 (IFI/Plenum, New York, 1972).
22. H.-J. Güntherodt, E. Hauser, H. U. Künzi, and R. Müller, *Phys. Lett. A* **54**:291 (1971).